Lava Lamp, a Novel Peripheral Golgi Protein, Is Required for *Drosophila melanogaster* Cellularization

John C. Sisson,* Christine Field,‡ Richard Ventura,* Anne Royou,§ and William Sullivan*

*Department of Molecular, Cell and Developmental Biology, Sinsheimer Labs, University of California at Santa Cruz, Santa Cruz, California 95064; ‡Department of Cell Biology, Harvard Medical School, Boston, Massachusetts 02115; and §Centre National de la Recherche Scientifique, Centre de Génétique Moléculaire, 91198 Gif sur Yvette, France

Abstract. *Drosophila* cellularization and animal cell cytokinesis rely on the coordinated functions of the microfilament and microtubule cytoskeletal systems. To identify new proteins involved in cellularization and cytokinesis, we have conducted a biochemical screen for microfilament/microtubule-associated proteins (MMAPs). 17 MMAPs were identified; seven have been previously implicated in cellularization and/or cytokinesis, including KLP3A, Anillin, Septins, and Dynamin. We now show that a novel MMAP, Lava Lamp (Lva), is also required for cellularization. Lva is a coiled-coil protein and, unlike other proteins previously implicated in cellularization or cytokinesis, it is Golgi associated. Our functional analysis shows that cellularization is dramatically inhibited upon injecting anti–Lva antibodies (IgG and Fab) into embryos. In addition, we show that brefeldin A, a potent inhibitor of membrane trafficking, also inhibits cellularization. Biochemical analysis demonstrates that Lva physically interacts with the MMAPs Spectrin and CLIP190. We suggest that Lva and Spectrin may form a Golgi-based scaffold that mediates the interaction of Golgi bodies with microtubules and facilitates Golgi-derived membrane secretion required for the formation of furrows during cellularization. Our results are consistent with the idea that animal cell cytokinesis depends on both actomyosin-based contraction and Golgi-derived membrane secretion.

Key words: cytokinesis • cytoskeleton • Spectrin • KLP3A • and brefeldin A

Introduction

Drosophila cellularization is a dramatic variation of animal cell cytokinesis (Foe et al., 1993; Schejter and Wieschaus, 1993; Miller and Kiehart, 1995). It transforms a one-cell syncytium into a multicellular embryo by simultaneously encapsulating roughly 5,000 cortical nuclei with one continuous plasma membrane furrow. The furrow invaginates between adjacent nuclei perpendicular to the cell surface, and then widens along its base to seal each nucleus off from the inner cytoplasm. Although the honeycomb-patterned cellularization furrow appears distinct from the ring-like cytokinesis furrow, the mechanisms underlying their formation are strikingly similar. The progression of each furrow depends on an actomyosin-based contractile apparatus associated with the leading edge of each furrow (Satterwhite and Pollard, 1992, and references therein; Crawford et al., 1998). In addition to microfilaments (F-actin) and myosin II, each contractile apparatus also consists of the putative stabilizing elements, Anillin (Field and Alberts, 1995), Septins (Fares et al., 1995; Field et al., 1996; Neufeld and Rubin, 1994), and formin homology proteins (Afshar et al., 2000). Furrow progression in each case also appears to rely on the export of intracellular membrane to the cell surface (Fullilove and Jacobson, 1971; Burgess et al., 1997; Conner and Wessel, 1999; Jantsch-Plunger and Glotzer, 1999).

While significant progress has been made towards understanding the assembly and function of the contractile apparatus, much less is known about the mechanism of membrane export (reviewed in Glotzer, 1997; Bowerman and Severson, 1999; Field et al., 1999; Hales et al., 1999). In *Xenopus,* it is well established that membrane is delivered during anaphase to the furrowing portion of the plasma membrane (Bluemink and de Laat, 1973; Byers and Armstrong, 1986; Drechsel et al., 1997), but the exact target along the furrow is uncertain (Byers and Armstrong, 1986; Leaf et al., 1990). At least some of the membrane is Golgi derived (Leaf et al., 1990); however, other sources

Address correspondence to Dr. John C. Sisson, Department of Molecular, Cell and Developmental Biology, Sinsheimer Labs, University of California at Santa Cruz, Santa Cruz, CA 95064. Tel.: (831) 459-3402. Fax: (831) 459-3139. E-mail: sisson@darwin.ucsc.edu

of membrane have also been implicated (Bluemink and de Laat, 1973). Regardless of the intracellular membrane source, microtubules (MTs)[1] appear to be required for its delivery (Danilchik et al., 1998). In the case of cellularization, neither the membrane source nor the modes of membrane delivery are known. However, the need for membrane export during cellularization is underscored by an increase in cell surface area (Fullilove and Jacobson, 1971), and the requirement for Syntaxin 1 (Burgess et al., 1997) and Dynamin (Swanson and Poodry, 1981), proteins implicated in membrane transport.

During both cellularization and cytokinesis, the coordination of the F-actin and MT cytoskeletal systems contributes to contraction and/or membrane export (Foe et al., 1993; Field et al., 1999). Although the precise mechanism of this dependency relationship is unknown, MTs may act as tracks for recruiting factors required for the establishment and/or maintenance of the contractile ring, or provide structural stability to the contractile ring late in cytokinesis. During cellularization, long MTs grow out from apically positioned centrosomes down over the surface of nuclei and project their plus ends into the embryos interior, forming "inverted baskets" around each nucleus (Foe et al., 1993). Throughout most of cellularization, the contractile apparatus appears to move down along these MTs as it leads the furrow inward at its tip (see Fig. 4, inset) (Foe et al., 1993). When embryos are treated with drugs that destabilize either F-actin or MTs during cellularization, furrow progression is severely disrupted (Zalokar and Erk, 1976; Foe and Alberts, 1983). The extent to which these treatments disrupt contraction versus membrane export is unknown.

We were interested in identifying new proteins involved in cellularization in order to better understand the mechanisms underlying cellularization and cytokinesis. Because the F-actin and MT cytoskeletal systems appear to intimately associate during cellularization, we set out to identify microfilament/microtubule-associated proteins (MMAPs) from *Drosophila* embryo extracts. This approach combines the methods of two previous biochemical screens for either F-actin– or MT-binding proteins in *Drosophila* (Kellogg et al., 1989; Miller et al., 1989). We have successfully isolated 21 MMAPs. Of these, 17 were identified and include seven proteins previously implicated in cellularization and/or cytokinesis, including KLP3A (Williams et al., 1995; Giansanti et al., 1998), Anillin (Field and Alberts, 1995; Giansanti et al., 1999), Septins (Neufeld and Rubin, 1994; Fares et al., 1995; Field et al., 1996), and Dynamin (Swanson and Poodry, 1980, 1981; Wienke et al., 1999). In addition, a novel protein, Lava Lamp (Lva), was identified. Our functional analysis of Lva indicates that it too is required for cellularization. Lva is Golgi associated and may function as part of a Spectrin-based scaffold. Our data suggests that MT-dependent, Golgi-derived membrane vesicle export is a key mechanism of *Drosophila* cellularization.

[1]*Abbreviations used in this paper:* ABP, actin-binding protein; BFA, brefeldin A; GST, glutathione-*S*-transferase; Lva, Lava Lamp; MHC, myosin heavy chain; MMAP, microfilament/microtubule-associated protein; MP, microprojection; MS/MS, tandem mass spectrometry analysis; MT, microtubule; Myo-GFP, myosin II–green fluorescent protein; PM, plasma membrane.

Materials and Methods

Fly Stocks and Culturing

A large-scale Oregon-R fly culture provided embryos for protein biochemistry and immunofluorescence (Sisson, 2000). The *sqh-gfp* transgenic stock was used for all live scanning confocal analysis (Royou et al., 1999).

Protein Purification and Chromatography

Actin was purified from rabbit skeletal muscle according to Pardee and Spudich (1982). Tubulin was purified from cow brain according to Mitchison and Kirschner (1984). Aliquots of G-actin and tubulin were frozen in liquid N_2 and stored at −80°C until needed.

The MMAPs were purified from 30 g of 1–3-h-old Oregon-R embryos. F-actin affinity chromatography was performed essentially as described by Miller et al. (1989). Approximately 400 mg of soluble protein (100,000 *g* supernatant, S100) was passed over two 7-ml BSA precolumns followed by two 7-ml phalloidin-stabilized, F-actin columns. After loading each BSA/F-actin column series, the columns were disconnected from one another, and the F-actin columns were washed extensively, and eluted with 1 mM ATP and 0.5 M KCl. The F-actin column eluates were pooled (actin-binding proteins, ABPs), dialyzed against MT-binding buffer [CX buffer (Kellogg et al., 1989) + 0.05% NP40], supplemented with 40 μm taxol, and clarified at 100,000 *g* for 1 h at 4°C. The supernatant was supplemented with preassembled, taxol-stabilized, 21-g needle-sheared MTs. The mixture was incubated at 24°C for 30 min, layered onto a 40% glycerol cushion (with 20 μm taxol), and centrifuged (30 min, 50,000 *g*, 25°C). The supernatant was removed, the pellet was thoroughly rinsed, resuspended, and resedimented as before in the presence of 40 μM taxol at 28°C for 30 min. The proteins resedimenting with MTs (MMAPs) were separated by SDS-PAGE, and six Coomassie-stained protein bands were excised and prepared for tandem mass spectrometry analysis (MS/MS, performed at Harvard Microchem). The remaining proteins were identified by immunoblot (see below).

A Superose 6 HR 10/30 FPLC column was used to fractionate 1.2 mg of S100 and 1.8 mg of the MMAP fraction, 0.5 ml fractions were analyzed by immunoblot.

For F-actin column rebinding, ABPs were dialyzed against fresh actin-binding buffer [A buffer (Miller et al., 1989) + 10% glycerol, and 50 mM KCl], and passed over a fresh 2 ml F-actin column. The column was extensively washed and eluted as before, and 0.25-ml fractions were analyzed by immunoblot.

ABP2/Lva cDNA and Antibody

An antisera raised to ABP2 (Miller et al., 1989) was used to screen a λgt11 expression library. A 3-kb cDNA clone (CF2) was isolated and sequenced according to Field and Alberts (1995). A 1.4-kb BamHI–EcoRI fragment from CF2 was ligated into the expression plasmid pGEX-3X (Amersham Pharmacia Biotech). The glutathione-*S*-transferase (GST)–Lva fusion protein was produced and purified according to the manufacture's protocol and used to immunize a rabbit (Babco). Antisera was affinity-purified according to Field and Alberts (1995). The affinity-purified antibody was used at 15 ng/ml for immunoblots and 0.1 μg/ml for immunofluorescence on fixed embryos. The antibody was concentrated using Ultrafree-MC columns according to the manufacturer's protocol (Millipore). The Fab fragments were prepared from affinity-purified anti–GST and anti–Lva IgGs according to Harlow and Lane (1988). Papain digested Fc fragments and undigested IgG were removed in batch with Affi-gel Protein A (Bio-Rad Laboratories), Fab fragments were dialyzed against 0.5× PBS, and concentrated as described above.

Other Primary Antibodies

Affinity-purified, rabbit polyclonal antibodies were used to detect CP60 and 190 (gifts of K. Oegema, EMBL, Heidelberg, Germany), kinesin heavy chain (gift of L. Goldstein, University of California at San Diego, La Jolla, CA), α- (#354) and β-Spectrin (#337) (gifts of D. Branton, Harvard University, Cambridge, MA), Dynamin (gift of M. McNiven, Mayo Foundation, Rochester, MN), Pnut and Sep2 (Field et al., 1996), Sep1 (gift of J. Pringle, University of North Carolina, Chapel Hill, NC), myosin heavy chain (MHC; Foe et al., 2000), and Anillin (Field and Alberts, 1995). Rabbit polyclonal antibodies were used to detect β_H-Spectrin (gift of G. Thomas, Pennsylvania State University, State College, PA), bifocal (gift of W. Chia, National University of Singapore, Kent Ridge, Sin-

gapore), KLP3A (No. 164, gift of M. Goldberg, Cornell University, Cornell, NY), β-COP (gift of V. Malhotra, University of California at San Diego, La Jolla, CA), LAGSE and HIPYR (pan-kinesin, gifts of J. Scholey, University of California, Davis, CA), and RFABG (gift of K. Kutty, National Institutes of Health, Bethesda, MD). Mouse monoclonal antibodies were used to detect 95F (3C7) and CLIP190 (gifts of K. Miller, Washington University, St. Louis, MO), actin (JLA20, DB Hybridoma Bank), dynein (gift of T. Hays, University of Minnesota, Minneapolis, MN), p120 (gift of V. Malhotra), and Tubulin (Sigma-Aldrich). A rat monoclonal was used to detect $p150^{Glued}$ (gift of T. Hays, University of Minnesota, Minneapolis, MN).

Immunoprecipitations

Affi-gel Protein A beads (Bio-Rad Laboratories) were washed with IP buffer (50 mM Hepes, pH 7.5, 0.5 mM EGTA, 0.5 mM EDTA, 0.05% NP40, and 150 mM KCl). Washed beads (20 μl) were incubated with either BSA (100 μg), affinity-purified anti–Lva (2.75 μg), monoclonal anti–CLIP190 (5 μl), or affinity-purified anti–α-Spectrin (5 μl) antibodies, and IP buffer in 100 μl final volume at 4°C for 4 h. Beads were pelleted, washed (8 × 800 μl), mixed with 300 μl MMAP fraction (diluted with IP buffer to 1 mg/ml), and incubated at 4°C for 4 h. The supernatant (S) was removed, the bead pellets (P) were washed as before, and samples were analyzed by immunoblot.

Electrophoresis and Immunoblotting

SDS-PAGE and immunoblotting were performed essentially as described by Kellogg et al. (1989). For optimum resolution, SDS-polyacrylamide [acryl:bis (100:1)] gradient (6.5–13.5%) gels were used. Proteins were transferred to nitrocellulose membrane (Schleicher & Schuell). Protein blots were rinsed with H_2O, Ponceau-S (Sigma-Aldrich) stained, and protein bands were marked with a wax pencil. Affinity-purified, HRP-conjugated goat antibodies against rabbit and mouse IgG (Santa Cruz Biotechnology, Inc.), and chemiluminescence reagent (ECL; Amersham Pharmacia Biotech) were used to detect primary antibodies. A coincident wax pencil mark on the blot and chemiluminescence signal on the film indicated that a protein band was composed of the protein detected.

Immunolocalization in Embryos

Oregon-R embryos were dechorionated as in Rothwell et al. (1999), quickly rinsed in 0.1% Triton X-100, and incubated in heptane for 45 s before adding an equal volume of 19.5% formaldehyde + 2.2–3.3% methanol. The embryos were fixed for 15–30 min at 25°C. Four different preparative conditions were also used: formalin for 5 min, 37.5% EM-grade paraformaldehyde (EM Sciences) for 5 min, heptane presaturated against 0.25% glutaraldehyde + methanol (1:1) for 30 min according to Thomas

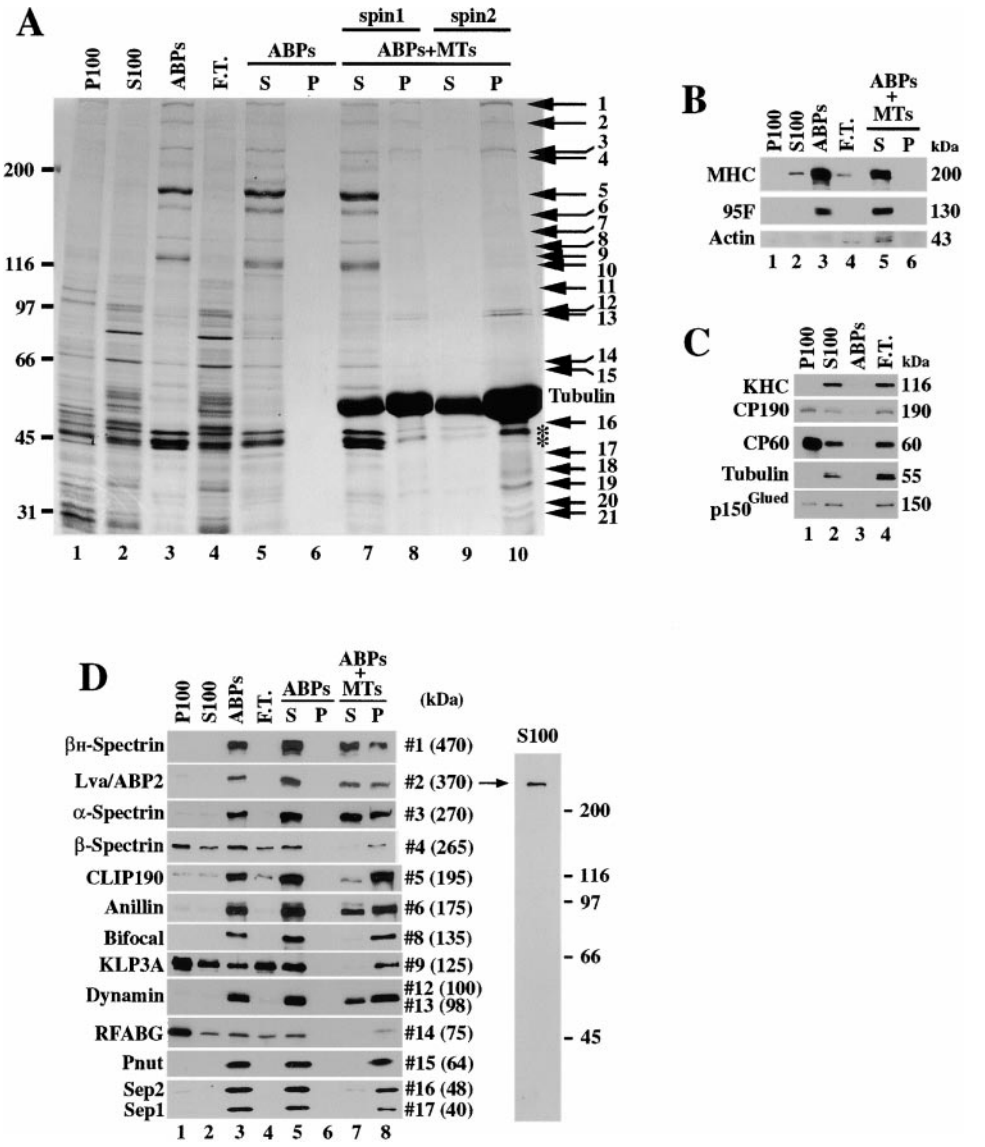

Figure 1. The purification of *Drosophila* MMAPs. (A) This Coomassie-stained SDS-polyacrylamide gradient gel shows the proteins within different fractions from the purification: high-speed pellet (P100) and supernatant (S100, column load), F-actin–binding proteins (ABPs), and F-actin column flow through (F.T.). Lanes 1–4 were each loaded with 25 μg of total protein. ABPs do not sediment without MTs (lanes 5 and 6), but a small subset of ABPs do sediment with MTs (spin 1). The lane 8 pellet was rinsed, resuspended, and the MTs were resedimented (spin 2). Numbered arrows indicate the proteins that resediment with the MTs. Comparable amounts of each matched supernatant (S) and pellet (P) were loaded. Molecular weight standards are indicated to the left. *Presumed protein degradation. (B) Immunoblots for MHC, 95F, and actin. Lanes are labeled and loaded as in A, lanes 5 and 6 correspond to spin 1 in A. (C) Immunoblots for the indicated MT-binding proteins, and tubulin. Each lane is labeled and loaded as in A. (D, left) Equivalent protein blots probed with antibodies to the indicated proteins. Each lane is labeled and loaded as in A. Coomassie-stained band numbers and molecular weights are indicated to the right. (Right) S100 (25 μg) protein blot probed with affinity-purified rabbit anti–Lva antibody. Molecular weight standards are indicated.

Table I. Summary of the Identified MMAPs

Coomassie band	Proteins detected	Detected by	Matching peptides	F-actin column binding	F-actin column rebinding	MT binding	Proposed function	References
1	β_H-Spectrin	IB	n.a.	Strong	Strong	Intermed.	Establish and/or maintain plasma membrane subdomains	Zarnescu and Thomas, 1999
2	Lva/ABP2	MS/MS and IB	64	Strong	Strong	Intermed.	Golgi-based secretion	This study
3	α-Spectrin	MS/MS and IB	61	Strong	Strong	Intermed.	Establish and/or maintain plasma membrane subdomains	Zarnescu and Thomas, 1999
	RFABG	MS/MS and IB	4	Weak	None	Strong	Transport of hydrophobic molecules	Kutty et al., 1996
4	β-Spectrin	IB	n.a.	Weak	Weak	Strong	Establish and/or maintain plasma membrane subdomains	Zarnescu and Thomas, 1999
5	CLIP190	IB	n.a.	Strong	Strong	Strong	Implicated in linking endocytic vesicles and organelles to MTs	Lantz and Miller, 1998; Rickard and Kreis, 1996
6	Anillin	IB	n.a.	Strong	Strong	Strong	Implicated in cytokinesis and cellularization	Field and Alberts, 1995; Giansanti et al., 1999
9	α-COP	MS/MS	5	?	?	?	Membrane vesicle transport	Flybase gene CG7961
	Bifocal	MS/MS and IB	2	Strong	Intermed.	Strong	Possible role in apical-basal plasma membrane polarity	Bahri et al., 1997
	MMAP140	MS/MS	14	?	?	?	Unknown	Flybase gene CG9805
10	KLP3A	IB	n.a.	Weak	None	Strong	Required for cytokinesis and pronuclear fusion	Giansanti et al., 1998; Williams et al., 1995, 1997
12	Dynamin	MS/MS and IB	24	Strong	None	Strong	Required for vesicle formation, cytokinesis, cellularization, and pole cell formation	Swanson and Poodry, 1980, 1981; Wienke et al., 1999; McNiven et al., 2000
13	Dynamin		29					
14	RFABG	MS/MS and IB	10	Weak	None	Strong	Transport of hydrophobic molecules	Kutty et al., 1996
15	Peanut	IB	n.a.	Strong	Strong	Strong	Required for cytokinesis and implicated in vesicle docking and/or targeting	Field and Kellogg, 1999
16	Septin 2				ND			
17	Septin 1				ND			

The number of unique tryptic peptides, derived from the predicted translations of DNA sequence, that match MS/MS data are indicated. Two proteins were detected in band 3, and three in band 9. The relative strength of F-actin and MT binding was determined by quantitative immunoblot. IB, Immunoblot; n.a., not analyzed; intermed., intermediate; ?, antibody unavailable; RFABG, retinoid and fatty acid–binding glycoprotein.

and Kiehart (1994), and our initial fixation method in the absence of Triton X-100 before or after the fix; otherwise, the post-fix treatment was according to Rothwell et al. (1999). Detection of plasma membrane (PM)-Spectrin requires post-fixation treatments with >0.5% Triton X-100, while Golgi-Spectrin requires 0.05% Triton X-100. Affinity-purified, goat anti–rabbit IgG-Cy5 and goat anti–mouse IgG-fluorescein antibodies (Chemicon) were used to detect primary antibodies. Embryos were imaged according to Rothwell et al. (1999).

Injections of Live Embryos

sqh-gfp embryos were prepared for microinjection and scanning confocal microscopy according to Francis-Lang et al. (1999). Injections were done at 50% egg length, on the dorsal side, within the first 5 min of nuclear cycle 14. The following reagents were injected: 50 μg/ml goat anti–rabbit IgG-Cy5 (Chemicon) mixed with either 0.25 mg/ml rabbit anti–GST or 0.3 mg/ml rabbit anti–Lva, 3.8 mg/ml rabbit anti–Lva, DMSO (Hybri-Max; Sigma-Aldrich), 50 mM BFA (Epicentre Technology), 25 mM colchicine, and 10 mM cytochalasin D. Final concentrations of BFA, colchicine, and cytochalasin D were ~1.5, 0.75, and 0.3 mM, respectively (Foe and Alberts, 1983). In syncytial, but not cellularizing blastoderms, DMSO alone can cause nuclei to move away from the cell surface. All injected antibodies were affinity purified. In the colchicine and cytochalasin D experiments, embryos were injected with the dilute, Cy5-tagged anti–Lva antibody within the first 2 min of cycle 14, confocal movie data was gathered, embryos were reinjected through the existing wound with either drug, and the movies were resumed. The focal plane in all movies is at the embryo's equator, ~5–10 μm along the embryo's surface from the site of injection. Scanning confocal movies were started within 2 min of each injection. Eight images were accumulated every 30 s for 70 min, at ~23.5°C. Fixation and immunofluorescence on antibody-injected embryos was done according to Sharp et al. (1999).

Results

21 Proteins Selectively Associate with F-Actin and MTs In Vitro

The initial step of the protein purification was to isolate actin-binding proteins by F-actin affinity chromatography. A high-speed supernatant of a *Drosophila* embryo extract was passed over an F-actin column, and after extensive washing, the column was eluted with buffer containing 1 mM ATP and 0.5 M KCl. After SDS-PAGE, Coomassie staining revealed ~50 polypeptide bands in the ABP fraction (Fig. 1 A, lane 3). Together, the ABPs comprise 0.5–1.0% of the total soluble protein passed over the F-actin column. Immunoblots demonstrate that two known ABPs, MHC and 95F, an unconventional Myosin VI, are highly enriched on the F-actin column, consistent with previous results (Fig. 1 B, lanes 2 and 3) (Miller et al., 1989). Conversely, the MT-binding proteins kinesin heavy chain, centrosomal protein (CP) 190, CP60, p150^{Glued}, and dynein, as well as tubulin, do not bind significantly to the F-actin column, indicating selective binding (Fig. 1 C, lanes 2 and 3; dynein not shown).

For the next step, the ABP fraction was dialyzed into MT-binding buffer and supplemented with taxol-stabilized MTs. The MTs and any associated proteins were then cosedimented by centrifugation. No proteins sedimented in the absence of MTs (Fig. 1 A, lanes 5 and 6); however, several proteins sedimented in the presence of MTs (Fig. 1 A, lanes 7 and 8). After the resuspension of the pellet, 21 proteins resediment with the MTs, indicating that their MT binding is robust (Fig. 1 A, lanes 9 and 10). These proteins have been designated MMAPs. Significantly, although MHC and 95F are abundant in the ABP fraction. neither cosediments with MTs, nor does actin (Fig. 1 B, lanes 5 and 6).

Seven MMAPs Are Involved in Cytokinesis and One Is Novel

17 of 21 proteins isolated were identified by MS/MS and/or immunoblotting with existing antibodies (Fig. 1 D and Table I). 15 of these proteins have known functions. Seven (Anillin, KLP3A, Dynamin A and B, Peanut, Septin 1, and Septin 2) have been previously implicated in cellularization and/or cytokinesis, suggesting that the screen has

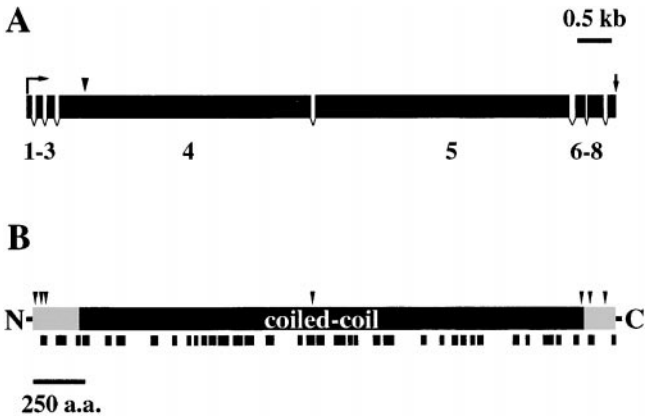

Figure 2. Molecular characterization of Lva. (A) The predicted gene structure shows exons (black rectangles) and introns (gaps). Exons are numbered 1–8. The gene prediction analysis was performed with the program FGENESH (available online from Baylor College of Medicine, Waco, TX). The positions of the putative start codon (bent arrow), stop codon (straight arrow), and the 5′ extent of the cDNA sequence (vertical arrowhead) are as indicated. (B) Lva is predicted to be globular at its termini (shaded) and form a coiled-coil along its central region (black). Arrowheads indicate the junctions between amino acids (a.a.) encoded by adjacent exons and the black marks below the diagram indicate the position of peptides matching MS/MS data.

enriched for the desired class of proteins. The function of Lva has not been previously reported. Notably, KLP3A, a member of the kinesin superfamily (Williams et al., 1995), was the only kinesin protein out of five detected in the S100 with pan-kinesin antibodies to bind the F-actin column at all (data not shown). CLIP190, a known partner of 95F (Lantz and Miller, 1998), was isolated in the absence of 95F. CLIP190 is the *Drosophila* homologue of human CLIP170 (Lantz and Miller, 1998), a protein implicated in linking vesicles and organelles to MT plus ends (Rickard and Kreis, 1996).

Lva Is a Novel Coiled-Coil Protein

We have focused our initial efforts on characterizing the novel protein, Lva. The mass spectra obtained from Lva perfectly match tryptic peptides derived from the translation product of a single predicted *Drosophila* gene, indicating that it encodes Lva (Fig. 2 B; CG#6450). The mass spectra match 64 tryptic peptides from seven of the eight predicted exons (Fig. 2, A and B). Tryptic peptides including the NH_2-terminal 18 amino acids, predicted to be encoded by exon 1, were not detected by MS/MS. However, the four nucleotides just upstream of the putative start codon of exon 1 are a good match to the *Drosophila* translational consensus sequence (Cavener, 1987), containing the invariant adenine at the −2 position, and stop codons exist in all reading frames just upstream of the putative start codon. cDNA sequence derived from a contiguous set of overlapping clones confirms the genomic DNA sequence from nucleotide 842 within exon 4 to the start of a poly(A) tail, 334 nucleotides downstream of the putative stop codon (Fig. 2 A). In addition, the cDNA sequence and MS/MS confirm the predicted intron/exon borders between exons 4–8 and 2–7, respectively. A full-length cDNA clone has not yet been identified.

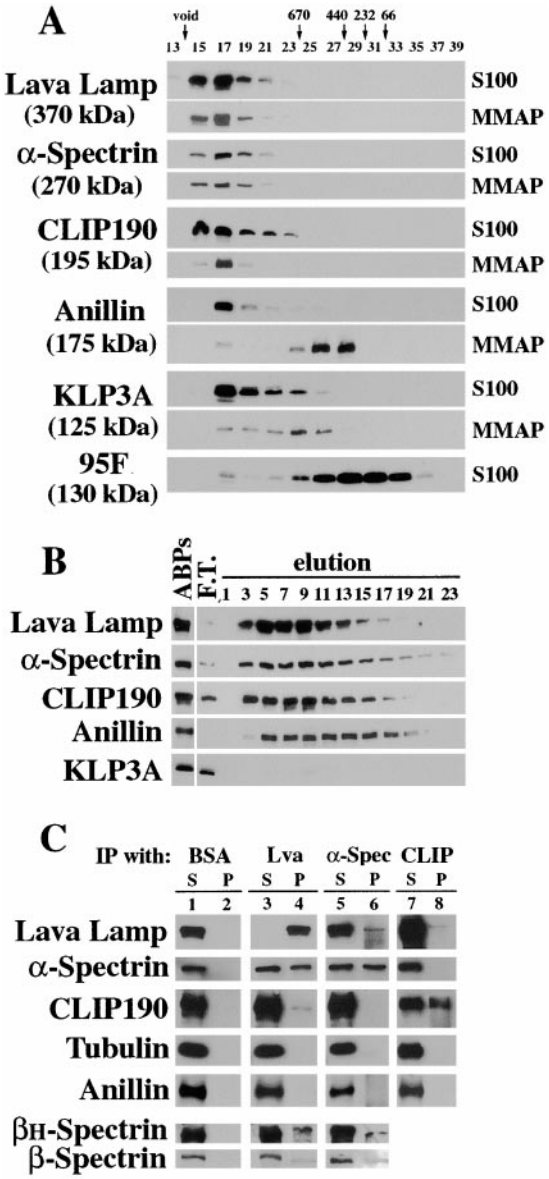

Figure 3. Lva associates with Spectrins and CLIP190. Immunoblots show (A) gel filtration elution profiles for the indicated proteins in the S100 and MMAP fractions. Fraction numbers and the elution peaks for native molecular weight standards are shown at the top. (B) Elution profiles for the indicated proteins that rebind an F-actin column. Lane headings indicate F-actin column load (ABPs), F-actin column flow through (F.T.), and elution fraction numbers. Identical results for each protein were also obtained with the MMAP fraction (data not shown). (C) A mock IP performed with BSA, and IPs performed with anti–Lva, anti–α-Spectrin, and anti–CLIP190 antibodies on the MMAP fraction. Proteins detected by immunoblot are indicated to the left. Comparable amounts of each matched supernatant (S) and pellet (P) were loaded.

The Lva gene is predicted to encode an acidic (pI 4.6) protein of 2,798 amino acids with a predicted molecular weight of 318 kD. Amino acid sequence analysis with COILS (Lupas et al., 1991) indicates that Lva is likely to form an extended coiled-coil (Fig. 2 B). Many rod-shaped proteins migrate slower than expected by SDS-PAGE, which may explain the discrepancy between the predicted

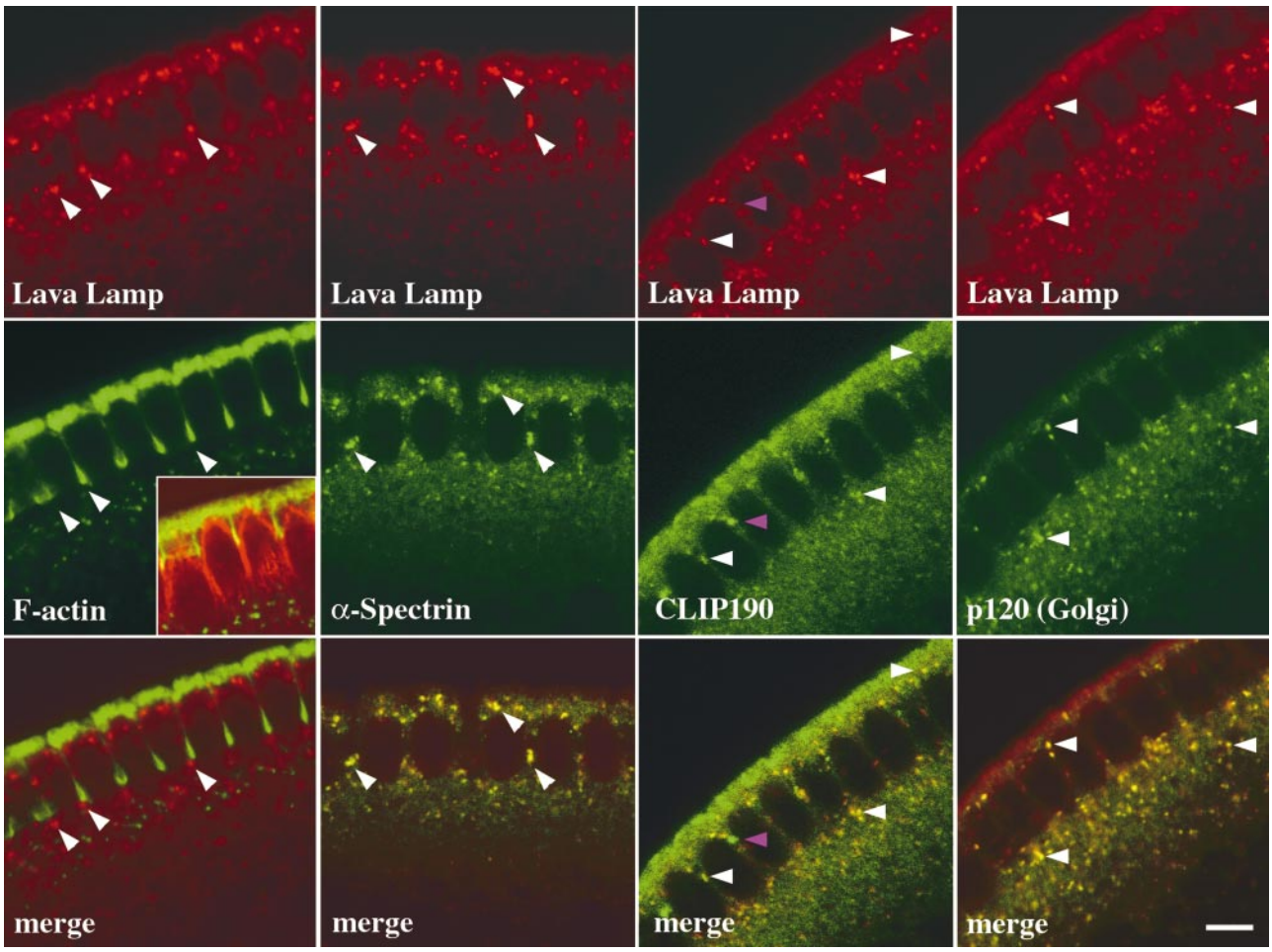

Figure 4. Lva, α-Spectrin, and CLIP190 colocalize to Golgi bodies. Cellularizing embryos were fixed, labeled with pairs of fluorescent probes, and examined by scanning confocal microscopy. From left to right, matched panels show Lva with F-actin, α-Spectrin, CLIP190, and the Golgi marker p120, respectively. White arrowheads indicate corresponding puncta in matched panels, except in the Lva/F-actin panels, where they indicate puncta at the furrow front. The purple arrowhead in the CLIP190 panel indicates CLIP190 with no corresponding Lva fluorescence. (Inset) Cortical F-actin (green) and MT-inverted baskets (red). Essentially no fluorescence was detected with secondary antibodies alone (data not shown). All views are sagittal. Bar, 5 μm.

and apparent molecular weights for Lva. Lva searches have not revealed homologues of Lva; however, BLAST does share features in common with golgins, a class of Golgi-associated proteins (see Discussion) (reviewed in Chan and Fritzler, 1998; Warren and Malhotra, 1998; Waters and Pfeffer, 1999).

While testing existing antibodies against our protein blots, we discovered that an antisera raised to *Drosophila* ABP2, a 370-kD F-actin–binding protein of unknown sequence (Miller et al., 1989), strongly reacts with Lva (Fig. 1 D). Moreover, a cDNA expression clone (CF2) isolated with the ABP2 antisera, is contiguous with Lva cDNA clones and matches Lva mass spectra. Therefore, ABP2 and Lva are products of the same gene. We will refer to the protein as Lva.

Lva Associates with Spectrins and CLIP190

To assess whether Lva interacts with other proteins, we first determined the native size of Lva compared with other MMAPs. The S100 and the final protein (MMAP) fraction were passed separately over a gel filtration column, and fractions were assayed by immunoblot. Because α-Spectrin has been previously shown to copurify with β- and β_H-Spectrin in two stable heterotetrameric complexes ($\alpha2\beta2$ and $\alpha2\beta_H2$, respectively) (Dubreuil et al., 1990) and coimmunoprecipitates with β- and β_H-Spectrin (Fig. 3 C), we will only present data for α-Spectrin for simplicity. Immunoblots show that in both the S100 and the MMAP fraction, Lva, CLIP190, αβ-, and $\alpha\beta_H$-Spectrin coelute from the column with native molecular weights larger then their predicted molecular weights, indicating that each protein exists in large, stable complexes (Fig. 3 A). By comparison, Anillin and KLP3A are initially present in large complexes that dissociate over the course of the purification (Fig. 3 A). The native molecular weight of Anillin in the final fraction is comparable with that observed for baculovirus-expressed, full-length frog Anillin (A. Straight, personal communication). Unlike the other proteins, most of 95F does not exist in a large complex in the S100 (Fig. 3 A).

Lva, CLIP190, αβ-, and $\alpha\beta_H$-Spectrin also cofractionate over two consecutive F-actin affinity columns, indicating that each protein is associated with a stable F-actin–bind-

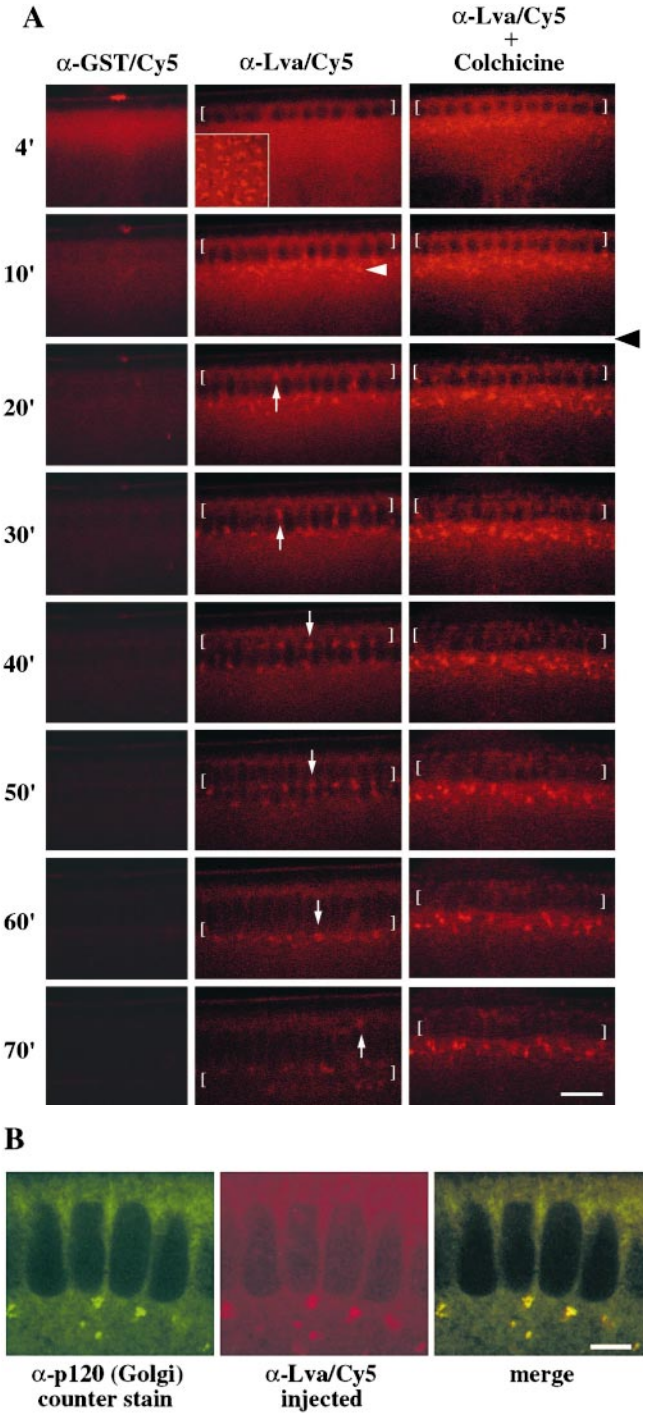

Figure 5. Golgi bodies undergo dynamic, MT-dependent movements in living embryos. (A) Frames from scanning confocal movies show three different Myo-GFP embryos injected at the start of cycle 14 with either diluted Cy5-tagged anti–GST (left), Cy5-tagged anti–Lva (center), or Cy5-tagged anti–Lva antibodies followed by injection of 25 mM colchicine 12.5 min into cycle 14 (right). The black arrowhead indicates the colchicine injection time. Brackets indicate the position of furrow fronts, arrows indicate the direction of Golgi movement (apical is up), and the white arrowhead indicates Cy5-marked Golgi bodies just basal of nuclei. Time (minutes) is relative to the start of cycle 14. The dorsal, injected surface of each embryo is shown. The inset shows a grazing view of pericentrosomal Golgi ~1.0 μm below the cell surface. All other views are sagittal. Bar, 10 μm. (B) Sagittal view of a cellularizing embryo that was injected with dilute, Cy5-tagged anti–Lva antibody (middle), fixed, and counter stained with anti–Golgi p120 antibody (left) with merged panel (right). Bar, 5 μm.

ing activity. S100 was passed over an F-actin column, ABPs were eluted as before, dialyzed against F-actin–binding buffer, and the soluble protein was passed over a second F-actin column. Immunoblots show that Lva, $\alpha\beta_H$-Spectrin, CLIP190, and Anillin each efficiently rebind the second column, while KLP3A does not (Fig. 3 B). The initial binding and subsequent rebinding of αβ-Spectrin to F-actin is relatively weak (Fig. 1 D and Table I), consistent with previous observations (Dubreuil et al., 1990). Lva, Spectrins, and CLIP190 elute with a common peak in fractions 5–9. In contrast, Anillin elutes more uniformly and slightly later then the others, reflecting a gel filtration effect and/or a difference in F-actin affinity. The rebinding of Anillin to the F-actin column is consistent with its known ability to bind F-actin directly (Field and Alberts, 1995). The exact nature of KLP3A's initial F-actin column binding is not yet known and may be conferred by another protein(s). Other MMAPs were also assayed (Table I).

Because Lva, CLIP190, and Spectrins, cofractionate in the above experiments, we assessed whether they interact by immunoprecipitation (IP). The IPs were performed on both the S100 and MMAP fraction, and because comparable results were obtained from each, only the results from the MMAP fraction are presented. Anti–Lva antibody efficiently precipitates Lva protein, and co-IPs $\alpha\beta_H$- and αβ-Spectrin, as well as CLIP190 (Fig. 3 C, lanes 3 and 4). Although the anti–α-Spectrin and anti–CLIP190 antibodies are inefficient at precipitating their respective antigens, both corroborate the co-IPs obtained with the anti–Lva antibody (Fig. 3 C, lanes 5–8). Although only a small portion of Lva and CLIP190 associate under our IP conditions, three controls suggest their association is specific. First, no proteins precipitate in the absence of specific antibody (Fig. 3 C, lanes 1 and 2). Second, although the exogenous (depolymerized) tubulin present in the MMAP fraction is in vast molar excess (Fig. 1 A, lane 10), no tubulin co-IPs with any of the antibodies tested (Fig. 3 C, compare all matched S and P). Third, anti–Lva antibody does not co-IP Anillin (Fig. 3 C, lanes 3 and 4), Dynamin, or Peanut (data not shown). Because antibodies to α-Spectrin and CLIP190 do not co-IP one another (Fig. 3 C, lanes 5–8), it is likely that Lva associates with Spectrins and CLIP190 separately.

Lva, α-Spectrin, and CLIP190 Are Golgi Associated

Blastoderm embryos were treated with fixatives that efficiently preserve both cortical F-actin and MTs and prepared for immunofluorescence (Foe et al., 2000). In syncytial and cellularizing blastoderms, Lva, α-Spectrin, and CLIP190 colocalize to large cytoplasmic puncta, some of which are found closely apposed to the furrow front in cellularizing blastoderms (Fig. 4, left, arrows). Additional CLIP190-specific puncta are also observed at furrow tips (Fig. 4, purple arrowhead). While most Lva is associated with puncta, low

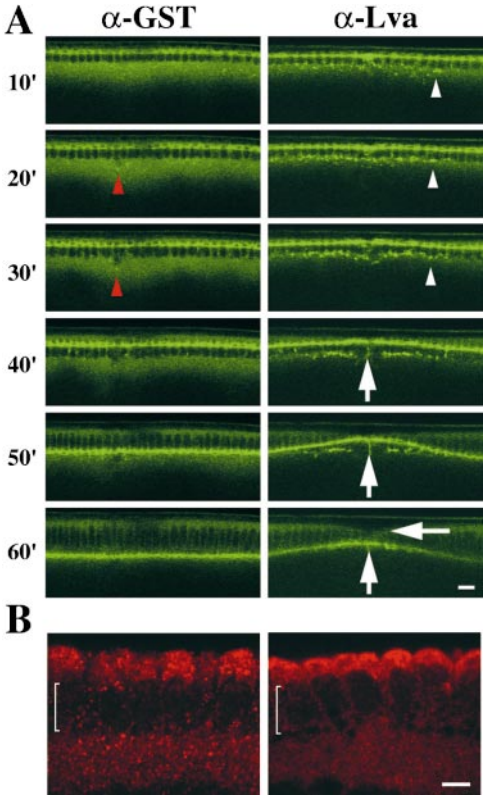

Figure 6. Anti–Lva IgG antibody inhibits furrow progression. All panels are from scanning confocal movies of Myo-GFP embryos. (A, left) Anti–GST antibody-injected embryo undergoing normal furrowing. The red arrowheads indicate an injection artifact that the embryo repairs. (Right) Anti–Lva IgG antibody (3.8 mg/ml)-injected embryo undergoing disrupted furrowing (vertical arrows). A surface dimple forms near the site of injection where furrowing is most impaired (horizontal arrow). The Myo-GFP puncta observed near the site of the anti–Lva antibody injection (white arrowheads) and the smaller Myo-GFP puncta observed normally in both embryos do not colocalize with anti–Lva/Cy5 antibody marked Golgi (data not shown). Time (minutes) is relative to the start of cycle 14. The dorsal, injected surface of each embryo is shown. All views are sagittal. Bar, 10 μm. (B) Sagittal views of two cellularizing embryos that were injected with either anti–GST (left) or anti–Lva (right) IgG antibodies, fixed, and stained with anti–Golgi p120 antibody. Brackets indicate the position of nuclei (apical is up). Bar, 5 μm.

levels are seen throughout the cortical cytoplasm. α-Spectrin and CLIP190 are also observed elsewhere within the cortical cytoplasm. Although α-Spectrin forms stable complexes with β- and β_H-Spectrin, we have not observed punctate β- or β_H-Spectrin localization. Instead, they are found throughout the cortical cytoplasm (data not shown). Unlike previous reports using different preparative methods (Thomas and Kiehart, 1994), we observe minimal Spectrin localization along the PM (see below).

Because the punctate colocalization pattern of Lva, α-Spectrin, and CLIP190 is reminiscent of that reported previously for two cis-Golgi markers, β-coatomer (β-COP) (Ripoche et al., 1994) and a 120-kD integral membrane protein (p120) (Stanley et al., 1997), we examined their distribution relative to the three MMAPs. Indeed, double immunofluorescence shows that p120 and Lva colocalize (Fig. 4, right). We have also found that α-Spectrin and CLIP190 colocalize with the Golgi markers, as with Lva (data not shown).

Although a special isoform of mammalian β-Spectrin (βIΣ-Spectrin) has been shown to associate with Golgi (reviewed in Beck and Nelson, 1998; De Matteis and Morrow, 1998), Golgi-associated Spectrin has not been previously described in *Drosophila*, where Spectrins have been shown primarily at the PM (Thomas and Williams, 1999, and references therein). To rule out fixation artifacts, we tested three different preparative conditions (see Materials and Methods). In each case, the punctate localization for α-Spectrin, Lva, and the Golgi markers was clearly observed, while very weak Spectrin localization was found at the PM (data not shown). However, when embryos were prepared for immunofluorescence according to the procedure of Thomas and Kiehart (1994), we observed all three Spectrins associated with the PM of cellularization furrows as previously described, while Lva remained Golgi associated (data not shown). Together, these results suggest that Spectrins reside on both the PM and Golgi bodies of cellularizing blastoderms, and that each Spectrin population is differentially sensitive to the immunofluorescence preparative conditions used (see Material and Methods, and Discussion).

Golgi Bodies Move Towards and Associate with the Furrow Front in Living Embryos

The Golgi bodies found positioned at the tips of cellularization furrows in fixed embryos suggested that some Golgi might specifically associate with the furrow. To assess this possibility, we observed Golgi in live cellularizing blastoderms using scanning confocal movies. Rabbit anti–GST and anti–Lva antibodies were diluted, indirectly labeled with anti–rabbit-Cy5 fluorescent antibodies, and injected separately into embryos at the start of cellularization. Upon injection, Cy5-tagged anti–GST antibody quickly diffuses (Fig. 5A). However, when the Cy5-tagged anti–Lva antibody is injected, Cy5 fluorescence quickly assumes a punctate distribution at the basal ends of nuclei (Fig. 5 A). Neither diluted antibody inhibits furrow progression. After the fixation of embryos injected with anti–Lva/Cy5 antibodies, the Cy5-marked puncta were found to perfectly colocalize with Golgi p120 by immunofluorescence, indicating that the Cy5-marked puncta are indeed Golgi bodies (Fig. 5 B). Although apically positioned Golgi bodies are not readily visible in sagittal views, grazing optical sections clearly show Cy5-marked Golgi bodies positioned apically of nuclei (Fig. 5 A, inset). The large amount of background Cy5 fluorescence appears to obscure the apical Golgi bodies when viewed sagittally.

The Cy5-marked Golgi undergo dramatic movements and associate with the furrow front during cellularization (Fig. 5 A). Cellularization begins during the 14 syncytial nuclear cycle (Foe et al., 1993). Initially, the furrow progresses slowly ("slow phase"), and then, ~40 min into nuclear cycle 14, the rate suddenly increases until the end of cellularization ("fast phase"). During the first 5–15 min of cycle 14, the Cy5-marked Golgi move in a saltatory manner at the base of nuclei. At ~20 min, individual Golgi bodies move apically and become closely associated with the furrow front, accumulating there over the next 10–20 min of the slow phase. Throughout the first 20–25 min of the fast phase, the Cy5-marked Golgi bodies remain intimately associated with the advancing furrow front. When the furrow front has progressed 5–8 μm beyond the basal ends of the nuclei, Golgi reverse their direction and move rapidly towards the cell

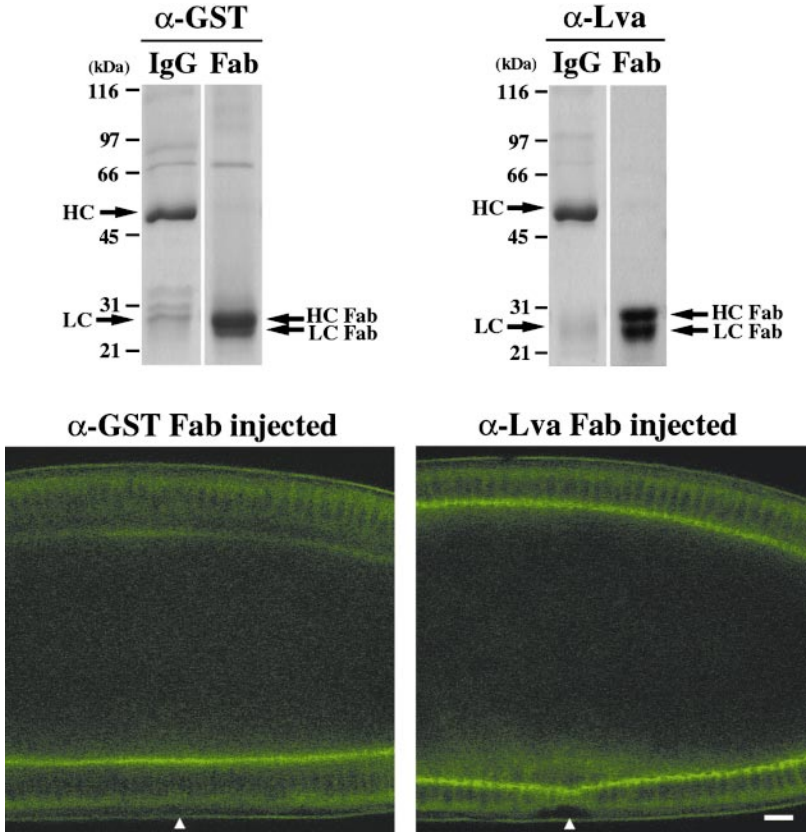

Figure 7. Anti–Lva Fab antibody inhibits furrow progression. (Top) Coomassie stained 10% SDS-polyacrylamide gels show affinity-purified anti–GST IgG and Fab antibodies (left), and affinity-purified anti–Lva IgG and Fab antibodies (right). About 5 μg of each sample was loaded in the presence of β-mercaptoethanol. Arrows indicate intact heavy chains (HC) and light chains (LC), in addition to heavy chain and light chain fragments, HC Fab and LC Fab, respectively. (Bottom) Two Myo-GFP embryos shown 65 min after being injected at the beginning of nuclear cycle 14 with either anti–GST Fab (5 mg/ml, left), or anti–Lva Fab (8.5 mg/ml, right) antibodies. The large Myo-GFP puncta observed in anti–Lva IgG-injected embryos are not observed in anti–Lva Fab antibody-injected embryos. The white arrowheads indicate the injection site. Views are sagittal. Bar, 10 μm.

surface again, increasing the total amount of Golgi within the apical cytoplasm. These apical/basal movements of the fluorescently marked Golgi bodies are identical to the movements of comparably sized organelles observed in living embryos by Nomarski DIC optics (Foe and Alberts, 1983), and resemble the motion of droplets in a lava lamp.

The Apically Directed Golgi Movement Is MT Dependent

The trajectory of the Golgi movements suggested it might be MT based. To test this possibility, we fluorescently marked Golgi bodies as before, and then after MT inverted-baskets formed, reinjected embryos with 25 mM colchicine either 15 or 25 min into cycle 14 to depolymerize MTs (Foe and Alberts, 1983; Zalokar and Erk, 1976). When colchicine was injected at 15 min, Golgi failed to move apically, instead accumulating along the basal ends of nuclei, and furrow progression was severely disrupted (Fig. 5 A), consistent with previous observations (Foe and Alberts, 1983; Zalokar and Erk, 1976). In embryos injected with colchicine at 25 min, Golgi bodies moved apically during the slow phase, but failed to do so during the fast phase, and furrow progression was only mildly effected (data not shown). Although furrow progression is severely inhibited upon injecting the F-actin destabilizing drug cytochalasin D early in cycle 14, Golgi bodies still move apically during the slow phase, as they do during the fast phase upon later injections that minimally affect furrow progression (data not shown). The organelles seen by Nomarski DIC optics display the identical pattern of MT-dependent, F-actin–independent movements in live cellularizing blastoderms (Foe and Alberts, 1983). We believe these particles are likely to be Golgi bodies.

Lva and Golgi Bodies Are Essential for Furrow Progression

Because no mutations are known to exist in the *lva* gene, we injected a concentrated preparation (3.8 mg/ml) of the anti–Lva antibody into embryos at the start of cycle 14 to block Lva function, and recorded the effects on Golgi bodies and furrow progression. To visualize the furrow front in these experiments, we used embryos bearing a *spaghetti squash* (*sqh*)–*green fluorescent protein* (*gfp*) transgene (Royou et al., 1999). *sqh* encodes the regulatory light chain of Myosin II, which normally accumulates at the furrow front (Karess et al., 1991). Likewise, in *sqh-gfp* embryos, functional myosin II-GFP (Myo-GFP) reveals the furrow front (Royou et al., 1999). The rate and extent of furrow progression is normal in control embryos injected with anti–GST antibody (Fig. 6 A). However, injections of the anti–Lva antibody cause severe furrowing defects (Fig. 6 A). At ~50 min into cycle 14, furrow progression is clearly inhibited near the site of injection, where the antibody is most concentrated (Fig. 6 A). Further from the injection site, furrowing occurs at a reduced rate. Approximately 60 min into cellularization, the embryo's surface near the site of injection begins to dimple, becoming pronounced 10 min later (Fig. 6 A). This effect is presumably due to the pulling force exerted by the contractile apparatus on the surface of the embryo where furrowing has failed. Dimpling was never observed in control embryos. To directly examine the effects of the anti–GST and anti–Lva antibodies on Golgi, some injected embryos were fixed and analyzed by immunofluorescence using the anti–p120 cis-Golgi antibody. In control anti–GST antibody injected embryos, a normal distribution of p120 is observed (Fig. 6 B, left). However, in embryos injected with the concentrated

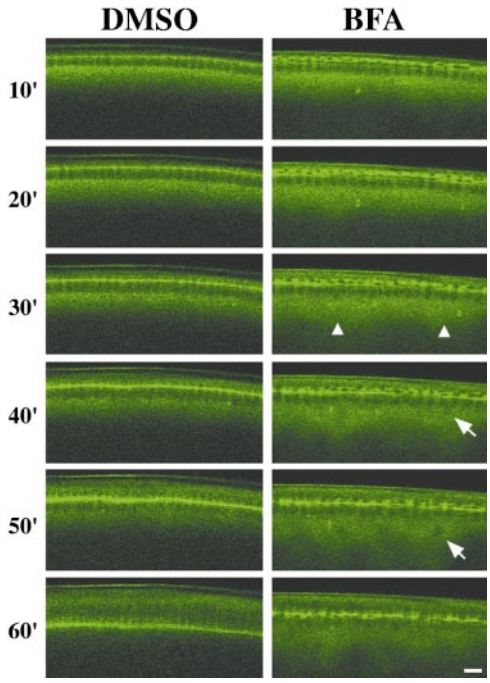

Figure 8. BFA inhibits furrow progression. (Left) DMSO-injected embryo undergoing normal furrowing. (Right) BFA-injected embryo displaying arrested furrowing at the fast phase. Arrowheads indicate unusually high levels of subcortical Myo-GFP, and arrows indicate a defective nucleus. Time (minutes) is relative to the start of cycle 14. The dorsal, injected surface of each embryo is shown. All views are sagittal. Bar, 10 μm.

anti–Lva antibody, the normal punctate distribution of p120 is not observed and instead p120 is found throughout the apical cytoplasm (Fig. 6 B, right). When the concentrated anti–Lva antibody is Cy5 tagged, the Lva protein can be seen to disperse within minutes of the injection, and the residual Lva protein left associated with some Golgi show them broken down and sessile (data not shown).

Furrow progression is also inhibited upon injecting monovalent anti–Lva Fab antibody, while injections of anti–GST Fab antibody has no effect (Fig. 7). The relatively uniform effect of the anti–Lva Fab antibody on furrow progression appears to result from the free diffusion of the antibody within the embryo, in contrast to the IgG, which remains concentrated near the site of injection. In addition, the anti–Lva Fab antibody does not induce the formation of Myo-GFP puncta, as seen with the anti–Lva IgG. This observation indicates that the formation of Myo-GFP puncta in anti–Lva IgG-injected embryos is not the cause of the furrowing inhibition.

Brefeldin A Inhibits Furrow Progression

The inhibition of furrow progression resulting from anti–Lva antibody injections suggested that Golgi-derived membrane vesicle export might be required for furrow progression. This predicts that the fungal toxin brefeldin A (BFA), a potent inhibitor of Golgi-derived membrane vesicle transport (Chardin and McCormick, 1999), should inhibit furrow progression. DMSO, the solvent for BFA, was injected into early Myo-GFP cellularizing blastoderms as a control, and no effect on furrowing was observed (Fig. 8). However, injection of BFA severely inhibits furrow progression (Fig. 8). Although the Myo-GFP at the furrow front appears discontinuous during the slow phase, furrow progression is relatively normal; however, the fast phase is absent. By 60 min, the furrows in BFA-injected embryos have invaginated only 50% as far as those in the control embryo (Fig. 8). When BFA is injected later, at ~25 min into cycle 14, furrow progression is only mildly affected (data not shown). Because BFA is a small, hydrophobic molecule (Chardin and McCormick, 1999), it diffuses rapidly through the embryo, resulting in a uniform effect.

Discussion

The Screen for MMAPs Has Identified Promising Candidates for Mediating and/or Using the F-Actin and MT Cytoskeletal Systems In Vivo

Drosophila cellularization, as well as several other fundamental cell processes, including cytokinesis, spindle positioning, vesicle transport, and cell movement, rely on the coordinated functions of the F-actin and MT cytoskeletal systems (Goode et al., 2000; Rogers and Gelfand, 2000). To understand the mechanisms by which these cytoskeletal systems are coordinated, it is necessary to identify the proteins involved. Although recent progress has been made towards this end, only a relatively modest number of candidate proteins have been identified (Fuchs and Yang, 1999; Goode et al., 2000). We have conducted a direct biochemical screen for *Drosophila* proteins that associate with both F-actin and MTs and have identified a set of proteins implicated in cellularization and/or cytokinesis, and membrane transport. Although the significance of the filament binding displayed by these MMAPs has not yet been established, some are promising candidates for mediating and/or using the F-actin and MT cytoskeletal systems during cellularization and/or cytokinesis. KLP3A is a particularly intriguing example in this regard. Although KLP3A is required for cytokinesis in *Drosophila* spermatocytes, it is not a true component of the contractile-ring. Instead, it specifically accumulates along interdigitating midzone MT bundles during anaphase, and is required for the assembly and/or maintenance of the contractile ring (Williams et al., 1995; Giansanti et al., 1998). We have shown that KLP3A associates with MTs, as expected for a kinesin, as well as F-actin. KLP3A was the only kinesin out of five detected to associate with the F-actin column. Its shift to a smaller molecular weight upon eluting the F-actin column correlates with a loss in F-actin binding, and suggests that another protein(s) may confer its F-actin binding. Together, these data are consistent with the possibility that KLP3A may associate with a component of the F-actin–rich contractile apparatus and participate in its recruitment during cytokinesis and cellularization. Our future studies will explore this possibility and assess the significance of the filament binding of other MMAPs.

Lva Resembles Golgins and May Form a Golgi-based Scaffold with Spectrin

Lva lacks significant overall sequence similarity to other proteins; however, it does resemble members of a growing class of proteins called golgins (Chan and Fritzler, 1998; Warren and Malhotra, 1998). Although golgins are themselves diverse with respect to size and sequence, they all

share two common protein features: each is predicted to form an extensive coiled-coil and associate with Golgi membrane. These are also defining features of Lva. Although the precise function of the golgins is unknown, recent work indicates that some golgins form a filamentous matrix between Golgi compartments, and Golgi compartments and COP I vesicles that may facilitate membrane budding and fusion, and maintain Golgi structural integrity (Warren and Malhotra, 1998; Waters and Pfeffer, 1999).

Two models have been proposed for how βIΣ-Spectrin might function on Golgi (Beck and Nelson, 1998; De Matteis and Morrow, 1998). Its principle role might be to specifically facilitate vesicle formation and/or transport by associating with adaptor complexes like COP I on donor membrane. Alternatively, it may form a dynamic scaffold over the Golgi's surface, which provides structural integrity and facilitates vesicle transport and cytoskeletal interactions. Because both golgins and Golgi-Spectrin may play structural roles, it has been suggested that they might interact and participate in some common Golgi functions (De Matteis and Morrow, 1998). Consistent with this proposal, we have established that Lva and Spectrins stably associate. In addition, upon injecting a specific anti–Lva antibody into cellularizing embryos, a dramatic redistribution of the cis-Golgi marker p120 occurs, MT-based Golgi movement is blocked, and furrow progression is severely inhibited. The most parsimonious explanation for these effects is that Lva forms part of a Golgi-based scaffold that supports MT interactions and membrane transport, including membrane vesicle export required for furrow progression. Interestingly, the distribution of p120 in embryos injected with the anti–Lva antibody closely resembles the normal distribution of the resident ER chaperone BiP (Lecuit and Wieschaus, 2000), suggesting that perhaps inhibition of Lva function blocks ER to Golgi membrane transport. Because we find Lva Golgi associated in *Drosophila* S2 cultured cells and in all embryonic cells examined (data not shown), we suspect Lva serves an essential Golgi function.

Lva and Spectrin might recruit MT-binding proteins to the surface of Golgi. Based on the rate (~0.1–0.2 μm/s) and direction of Golgi movement, it is possible that cytoplasmic dynein or a minus-end–directed kinesin are responsible. Interestingly, the mammalian dynactin complex has recently been shown to associate with Golgi via Spectrin (Holleran et al., 1996). In addition, CLIP170, the human homologue of CLIP190, has been found to specifically recruit dynactin to the plus-ends of MTs (Valetti et al., 1999; Vaughan et al., 1999). Although dynein and $p150^{Glued}$ do not appear to form a stable association with Spectrins in our experiments, a small proportion of CLIP190 and Lva stably associate and colocalize to Golgi bodies. These observations raise the possibility that CLIP190 and the dynactin complex may participate in linking Golgi to MTs during cellularization through Golgi-Spectrin or perhaps a transient association with the Lva/Spectrin complex that was not detected by our co-IP experiments.

Interestingly, the final wave of MT-dependent Golgi movement that we have observed from the furrow front to the apical cytoplasm perfectly coincides with a shift in the position of PM junctions from the basal furrow front to the apical furrow wall (Bhat et al., 1999; Thomas and Williams, 1999). Because polarized secretion is required for apical/basal cell polarity in mammalian epithelia (Drubin and Nelson, 1996), it is possible that the apical Golgi movements control the dynamic shift in the position of junctions during cellularization in *Drosophila*. The final wave of Golgi movement may also represent an efficient strategy for gathering Golgi into forming cells before the end of cellularization.

α-Spectrin Is Golgi Associated

By using fixation methods optimized for the preservation of both MTs and F-actin, we have found that α-Spectrin associates with Golgi bodies in blastoderm embryos. To our knowledge, this is the first demonstration of a Golgi-associated Spectrin in invertebrate cells, and the first instance of Golgi-associated α-Spectrin in any cell. Our findings suggest that while mammalian cells have a Golgi-specific isoform of β-Spectrin (Beck and Nelson, 1998; De Matteis and Morrow, 1998), *Drosophila* blastoderms appear to distribute the same α-Spectrin to both the PM and Golgi. Whether a special posttranslational modification of α-Spectrin confers its Golgi localization is unknown. However, PM- and Golgi-Spectrin are distinctly sensitive to immunofluorescent preparations, indicating that they may possess some compositional differences, certainly the association between Golgi-Spectrin and Lva is apparently one difference. The sensitivity of Golgi-Spectrin to these preparative conditions may explain why Golgi-Spectrin has not been previously described in *Drosophila*, and why we do not detect either β- or $β_H$-Spectrin on Golgi.

Golgi-derived Membrane Vesicle Export Is Essential for Cellularization

The source of membrane for cellularization has been controversial. One idea is that PM microprojections (MPs) observed above nuclei before furrow formation flatten to give rise to the furrow (Fullilove and Jacobson, 1971; Turner and Mahowald, 1977). The MPs could represent pre-existing PM that is thrown into patches of villi by cortical contraction, and/or they may result from de novo intracellular membrane delivery early during cellularization (Fullilove and Jacobson, 1971; Turner and Mahowald, 1977). In either case, estimates suggest the MPs can only account for one half of the total membrane required for furrowing; thus, the remaining membrane must come from intracellular stores (Fullilove and Jacobson, 1971), and numerous sources have been proposed (Fullilove and Jacobson, 1971; Sanders, 1975; Loncar and Singer, 1995; Lecuit and Wieschaus, 2000).

Together, several of our observations indicate that Golgi-derived membrane export is essential for cellularization. First, the association between Golgi bodies and the furrow front in live embryos suggests the Golgi may provide membrane to the furrow front through short-range vesicle delivery, consistent with previous EM data (Fullilove and Jacobson, 1971). In addition, the severity of the furrowing defects induced by the anti–Lva IgG and Fab fragments and BFA suggests that Golgi bodies are a significant source, and perhaps the principle source, of membrane for furrow progression.

Although both the slow and fast phases of furrow progression appear to depend on Lva function, the fast phase appears to be particularly sensitive to BFA. This may reflect a difference in the specific mechanism of exocytosis for each phase of furrow progression. For example, furrow progression during the slow phase, which precedes the fast

phase, may simply rely on pre-existing Golgi membrane stores, while the fast phase depends on BFA-sensitive active transport from the ER to Golgi. The timing of the BFA sensitivity is consistent with the proposal that membrane required for the fast phase is actually exported to the cell surface early during cycle 14 and "stored" in the form of MPs until the onset of the fast phase, when it is used to complete furrow progression (Turner and Mahowald, 1977). Lecuit and Wieschaus (2000) have recently obtained additional evidence supporting this possibility.

Perspectives

For over two decades, the generally accepted view of animal cell cytokinesis has been that an actomyosin-based contractile ring provides annular force, which, like a "purse-string," pulls the plasma membrane inward to form a cleavage furrow. However, evidence presented here, in addition to other recent studies showing that Syntaxin (Burgess et al., 1997; Conner and Wessel, 1999; Jantsch-Plunger and Glotzer, 1999) and phosphatidylinositol 4-kinase (Brill et al., 2000) are required for cytokinesis, indicate that the mechanism of animal cell cytokinesis is more complex and requires targeted membrane secretion. Our results extend these previous observations by directly showing that active Golgi-derived membrane vesicle secretion is essential for cytokinesis. Therefore, a more accurate paradigm for animal cell cytokinesis includes both actomyosin-based contraction and membrane vesicle secretion. Although this revised model does not diminish the importance of the contractile ring, it does raise an important question concerning its precise function. Namely, does the contractile ring provide driving force for cytokinesis, as commonly thought, or elastic force, which accommodates and guides new plasma membrane in the formation of a cleavage furrow? This newer perspective also leads to changes in the way we view the functions of proteins already known to be required for cytokinesis. For instance, the Septins associate with the contractile ring and have been proposed to recruit and/or stabilize the contractile ring. However, recently the mammalian Septins have been shown to physically associate with the Sec6/8 complex (Hsu et al., 1998) and Syntaxin (Beites et al., 1999), proteins implicated in polarized secretion and membrane vesicle fusion, respectively. So, perhaps the role of the Septin complex during cytokinesis is to facilitate the proper docking and/or fusion of membrane vesicles with the cleavage furrow. These and other considerations will undoubtedly become the subject of future work. Our current study has laid a basic foundation for future investigations in *Drosophila*, and will hopefully lead to a better understanding of how contraction and membrane secretion combine to bring about cytokinesis and other dramatic changes in cell shape.

We thank B. Alberts, T. Mitchison, O. Papoulas, V. Foe, J. Tamkun, G. Thomas, D. Kellogg, J. Moffat, and G. Hertzog for their helpful comments and advice, R. Karess for kindly sharing the *sqh*-GFP stock, V. Foe for her excellent fixation protocol, and J. Cordeiro for superb technical support. We also thank the following people for kindly providing antibodies: V. Malhotra, K. Miller, G. Thomas, D. Branton, B. Chia, M. Goldberg, M. McNiven, K. Kutty, L. Goldstein, T. Hays, J. Scholey, J. Pringle, and K. Oegema.

This work was supported by grants to J.C. Sisson (1F32GM19200-01), T. Mitchison and C. Field (GM23928), and W. Sullivan (GM46409-08) from the National Institutes of Health, and to A. Royou and R. Karess from le Ministère de l'Éducation Nationale de la Recherche et de la Technologie and the Centre National de la Recherche Scientifique (France).

Submitted: 24 August 2000
Revised: 26 September 2000
Accepted: 28 September 2000

References

Afshar, K., B. Stuart, and S.A. Wasserman. 2000. Functional analysis of the *Drosophila* Diaphanous FH protein in early embryonic development. *Development (Camb.)*. 127:1887–1897.

Bahri, S.M., X. Yang, and W. Chia. 1997. The *Drosophila bifocal* gene encodes a novel protein which colocalizes with actin and is necessary for photoreceptor morphogenesis. *Mol. Cell. Biol.* 17:5521–5529.

Beck, K.A., and W.J. Nelson. 1998. A spectrin membrane skeleton of the Golgi complex. *Biochim. Biophys. Acta.* 1404:153–160.

Beites, C.L., H. Xie, R. Bowser, and W.S. Trimble. 1999. The septin CDCrel-1 binds syntaxin and inhibits exocytosis. *Nat. Neurosci.* 2:434–439.

Bhat, M.A., S. Izaddoost, Y. Lu, K.O. Cho, K.W. Choi, and H.J. Bellen. 1999. Discs Lost, a novel multi-PDZ domain protein, establishes and maintains epithelial polarity. *Cell.* 96:833–845.

Bluemink, J.G., and S.W. de Laat. 1973. New membrane formation during cytokinesis in normal and cytochalasin B-treated eggs of *Xenopus laevis*. I. Electron microscope observations. *J. Cell Biol.* 59:89–108.

Bowerman, B., and A.F. Severson. 1999. Cell division: plant-like properties of animal cell cytokinesis. *Curr. Biol.* 9:R658–R660.

Brill, J.A., G.R. Hime, M. Scharer-Schuksz, and M.T. Fuller. 2000. A phospholipid kinase regulates actin organization and intercellular bridge formation during germline cytokinesis. *Development (Camb.)*. 127:3855–3864.

Burgess, R.W., D.L. Deitcher, and T.L. Schwarz. 1997. The synaptic protein syntaxin1 is required for cellularization of *Drosophila* embryos. *J. Cell Biol.* 138:861–875.

Byers, T.J., and P.B. Armstrong. 1986. Membrane protein redistribution during *Xenopus* first cleavage. *J. Cell Biol.* 102:2176–2184.

Cavener, D.R. 1987. Comparison of the consensus sequence flanking translational start sites in *Drosophila* and vertebrates. *Nucleic Acids Res.* 15:1353–1361.

Chan, E., and M.J. Fritzler. 1998. Golgins: coiled-coil-rich proteins associated with the Golgi Complex. *Elec. J. Biotech.* 1:1–10.

Chardin, P., and F. McCormick. 1999. Brefeldin A: the advantage of being uncompetitive. *Cell.* 97:153–155.

Conner, S.D., and G.M. Wessel. 1999. Syntaxin is required for cell division. *Mol. Biol. Cell.* 10:2735–2743.

Crawford, J.M., N. Harden, T. Leung, L. Lim, and D.P. Kiehart. 1998. Cellularization in *Drosophila melanogaster* is disrupted by the inhibition of rho activity and the activation of Cdc42 function. *Dev. Biol.* 204:151–164.

Danilchik, M.V., W.C. Funk, E.E. Brown, and K. Larkin. 1998. Requirement for microtubules in new membrane formation during cytokinesis of *Xenopus* embryos. *Dev. Biol.* 194:47–60.

De Matteis, M.A., and J.S. Morrow. 1998. The role of ankyrin and spectrin in membrane transport and domain formation. *Curr. Opin. Cell Biol.* 10:542–549.

Drechsel, D.N., A.A. Hyman, A. Hall, and M. Glotzer. 1997. A requirement for Rho and Cdc42 during cytokinesis in *Xenopus* embryos. *Curr. Biol.* 7:12–23.

Drubin, D.G., and W.J. Nelson. 1996. Origins of cell polarity. *Cell.* 84:335–344.

Dubreuil, R.R., T.J. Byers, C.T. Stewart, and D.P. Kiehart. 1990. A beta-spectrin isoform from *Drosophila* (beta H) is similar in size to vertebrate dystrophin. *J. Cell Biol.* 111:1849–1858.

Fares, H., M. Peifer, and J.R. Pringle. 1995. Localization and possible functions of *Drosophila* septins. *Mol. Biol. Cell.* 6:1843–1859.

Field, C., R. Li, and K. Oegema. 1999. Cytokinesis in eukaryotes: a mechanistic comparison. *Curr. Opin. Cell Biol.* 11:68–80.

Field, C.M., O. al-Awar, J. Rosenblatt, M.L. Wong, B. Alberts, and T.J. Mitchison. 1996. A purified *Drosophila* septin complex forms filaments and exhibits GTPase activity. *J. Cell Biol.* 133:605–616.

Field, C.M., and B.M. Alberts. 1995. Anillin, a contractile ring protein that cycles from the nucleus to the cell cortex. *J. Cell Biol.* 131:165–178.

Field, C.M., and D. Kellogg. 1999. Septins: cytoskeletal polymers or signalling GTPases? *Trends Cell Biol.* 9:387–394.

Foe, V.E., and B.M. Alberts. 1983. Studies of nuclear and cytoplasmic behaviour during the five mitotic cycles that precede gastrulation in *Drosophila* embryogenesis. *J. Cell Sci.* 61:31–70.

Foe, V.E., C.M. Field, and G.M. Odell. 2000. Microtubules and mitotic cycle phase modulate spatiotemporal distributions of F-actin and myosin II in *Drosophila* syncytial blastoderm embryos. *Development (Camb.)*. 127:1767–1787.

Foe, V.E., G. Odell, and B.A. Edgar. 1993. Mitosis and morphogenesis in the *Drosophila* embryo: point and counterpoint. *In* The Development of *Drosophila melanogaster*. M. Bate and A. Martinez Arias, editors. Cold Spring Harbor Laboratory Press, Cold Spring Harbor, NY. 149–300.

Francis-Lang, H., J. Minden, W. Sullivan, and K. Oegema. 1999. Live confocal analysis with fluorescently labeled proteins. *Methods Mol. Biol.* 122:223–239.

Fuchs, E., and Y. Yang. 1999. Crossroads on cytoskeletal highways. *Cell.* 98: 547–550.

Fullilove, S.L., and A.G. Jacobson. 1971. Nuclear elongation and cytokinesis in

Drosophila montana. *Dev. Biol.* 26:560–577.
Giansanti, M.G., S. Bonaccorsi, and M. Gatti. 1999. The role of *anillin* in meiotic cytokinesis of *Drosophila* males. *J. Cell Sci.* 112:2323–2334.
Giansanti, M.G., S. Bonaccorsi, B. Williams, E.V. Williams, C. Santolamazza, M.L. Goldberg, and M. Gatti. 1998. Cooperative interactions between the central spindle and the contractile ring during *Drosophila* cytokinesis. *Genes Dev*. 12:396–410.
Glotzer, M. 1997. The mechanism and control of cytokinesis. *Curr. Opin. Cell Biol.* 9:815–823.
Goode, B.L., D.G. Drubin, and G. Barnes. 2000. Functional cooperation between the microtubule and actin cytoskeletons. *Curr. Opin. Cell Biol.* 12:63–71.
Hales, K.G., E. Bi, J.Q. Wu, J.C. Adam, I.C. Yu, and J.R. Pringle. 1999. Cytokinesis: an emerging unified theory for eukaryotes? *Curr. Opin. Cell Biol*. 11:717–725.
Harlow, E., and D. Lane. 1988. Antibodies: A Laboratory Manual. Cold Spring Harbor Laboratory Press, Cold Spring Harbor, NY. 626–629.
Holleran, E.A., M.K. Tokito, S. Karki, and E.L. Holzbaur. 1996. Centractin (ARP1) associates with spectrin revealing a potential mechanism to link dynactin to intracellular organelles. *J. Cell Biol.* 135:1815–1829.
Hsu, S.C., C.D. Hazuka, R. Roth, D.L. Foletti, J. Heuser, and R.H. Scheller. 1998. Subunit composition, protein interactions, and structures of the mammalian brain sec6/8 complex and septin filaments. *Neuron*. 20:1111–1122.
Jantsch-Plunger, V., and M. Glotzer. 1999. Depletion of *syntaxins* in the early *Caenorhabditis elegans* embryo reveals a role for membrane fusion events in cytokinesis. *Curr. Biol*. 9:738–745.
Karess, R.E., X.J. Chang, K.A. Edwards, S. Kulkarni, I. Aguilera, and D.P. Kiehart. 1991. The regulatory light chain of nonmuscle myosin is encoded by *spaghetti-squash*, a gene required for cytokinesis in *Drosophila*. *Cell*. 65: 1177–1189.
Kellogg, D.R., C.M. Field, and B.M. Alberts. 1989. Identification of microtubule-associated proteins in the centrosome, spindle, and kinetochore of the early *Drosophila* embryo. *J. Cell Biol.* 109:2977–2991.
Kutty, R.K., G. Kutty, R. Kambadur, T. Duncan, E.V. Koonin, I.R. Rodriguez, W.F. Odenwald, and B. Wiggert. 1996. Molecular characterization and developmental expression of a retinoid- and fatty acid–binding glycoprotein from *Drosophila*. A putative lipophorin. *J. Biol. Chem.* 271:20641–20649.
Lantz, V.A., and K.G. Miller. 1998. A class VI unconventional myosin is associated with a homologue of a microtubule-binding protein, cytoplasmic linker protein-170, in neurons and at the posterior pole of *Drosophila* embryos. *J. Cell Biol.* 140:897–910.
Leaf, D.S., S.J. Roberts, J.C. Gerhart, and H.P. Moore. 1990. The secretory pathway is blocked between the trans-Golgi and the plasma membrane during meiotic maturation in *Xenopus* oocytes. *Dev. Biol.* 141:1–12.
Lecuit, T., and E. Wieschaus. 2000. Polarized insertion of new membrane from a cytoplasmic reservoir during cleavage of the *Drosophila* embryo. *J. Cell Biol*. 150:849–860.
Loncar, D., and S.J. Singer. 1995. Cell membrane formation during the cellularization of the syncytial blastoderm of *Drosophila*. *Proc. Natl. Acad. Sci. USA*. 92:2199–2203.
Lupas, A., M. Van Dyke, and J. Stock. 1991. Predicting coiled coils from protein sequences. *Science*. 252:1162–1164.
McNiven, M.A., I. Cao, K.R. Pitts, and I. Yoon. 2000. The dynamin family of mechanoenzymes: pinching in new places. *Trends Biochem. Sci.* 25:115–120.
Miller, K.G., C.M. Field, and B.M. Alberts. 1989. Actin-binding proteins from *Drosophila* embryos: a complex network of interacting proteins detected by F-actin affinity chromatography. *J. Cell Biol.* 109:2963–2975.
Miller, K.G., and D.P. Kiehart. 1995. Fly division. *J. Cell Biol.* 131:1–5.
Mitchison, T., and M. Kirschner. 1984. Microtubule assembly nucleated by isolated centrosomes. *Nature*. 312:232–237.
Neufeld, T.P., and G.M. Rubin. 1994. The *Drosophila peanut* gene is required for cytokinesis and encodes a protein similar to yeast putative bud neck filament proteins. *Cell*. 77:371–379.
Pardee, J.D., and J.A. Spudich. 1982. Purification of muscle actin. *Methods Enzymol.* 85:164–181.
Rickard, J.E., and T.E. Kreis. 1996. CLIPs for organelle-microtubule interactions. *Trends Cell Biol.* 6:178–183.
Ripoche, J., B. Link, J.K. Yucel, K. Tokuyasu, and V. Malhotra. 1994. Location of Golgi membranes with reference to dividing nuclei in syncytial *Drosophila* embryos. *Proc. Natl. Acad. Sci. USA*. 91:1878–1882.
Rogers, S.L., and V.I. Gelfand. 2000. Membrane trafficking, organelle transport, and the cytoskeleton. *Curr. Opin. Cell Biol.* 12:57–62.
Rothwell, W.F., C.X. Zhang, C. Zelano, T.S. Hsieh, and W. Sullivan. 1999. The *Drosophila* centrosomal protein Nuf is required for recruiting Dah, a membrane associated protein, to furrows in the early embryo. *J. Cell Sci.* 112: 2885–2893.
Royou, A., W. Sullivan, and R.E. Karess. 1999. *In vivo* studies of *Drosophila* nonmuscle myosin II tagged with green fluorescent protein. *Mol. Biol. Cell.* 10:34a.
Sanders, E.J. 1975. Aspects of furrow membrane formation in the cleaving *Drosophila* embryo. *Cell Tissue Res.* 156:463–474.
Satterwhite, L.L., and T.D. Pollard. 1992. Cytokinesis. *Curr. Opin. Cell Biol*. 4:43–52.
Schejter, E.D., and E. Wieschaus. 1993. Functional elements of the cytoskeleton in the early *Drosophila* embryo. *Annu. Rev. Cell Biol.* 9:67–99.
Sharp, D.J., K.R. Yu, J.C. Sisson, W. Sullivan, and J.M. Scholey. 1999. Antagonistic microtubule-sliding motors position mitotic centrosomes in *Drosophila* early embryos. *Nat. Cell Biol.* 1:51–54.
Sisson, J.C. 2000. Culturing large populations of *Drosophila* for protein biochemistry. *In Drosophila* Protocols: A Laboratory Manual. W. Sullivan, M. Ashburner, and S. Hawley, editors. Cold Spring Harbor Laboratory Press, Cold Spring Harbor, NY.
Stanley, H., J. Botas, and V. Malhotra. 1997. The mechanism of Golgi segregation during mitosis is cell type-specific. *Proc. Natl. Acad. Sci. USA*. 94:14467–14470.
Swanson, M., and C. Poodry. 1981. The *shibire* mutant of *Drosophila*: a probe for the study of embryonic development. *Dev. Biol.* 84:465–470.
Swanson, M.M., and C.A. Poodry. 1980. Pole cell formation in *Drosophila melanogaster*. *Dev. Biol.* 75:419–430.
Thomas, G.H., and D.P. Kiehart. 1994. Beta heavy-spectrin has a restricted tissue and subcellular distribution during *Drosophila* embryogenesis. *Development (Camb.)*. 120:2039–2050.
Thomas, G.H., and J.A. Williams. 1999. Dynamic rearrangement of the spectrin membrane skeleton during the generation of epithelial polarity in *Drosophila*. *J. Cell Sci.* 112:2843–2852.
Turner, F.R., and A.P. Mahowald. 1977. Scanning electron microscopy of *Drosophila melanogaster* embryogenesis. II. Gastrulation and segmentation. *Dev. Biol.* 57:403–416.
Valetti, C., D.M. Wetzel, M. Schrader, M.J. Hasbani, S.R. Gill, T.E. Kreis, and T.A. Schroer. 1999. Role of dynactin in endocytic traffic: effects of dynamitin overexpression and colocalization with CLIP-170. *Mol. Biol. Cell*. 10: 4107–4120.
Vaughan, K.T., S.H. Tynan, N.E. Faulkner, C.J. Echeverri, and R.B. Vallee. 1999. Colocalization of cytoplasmic dynein with dynactin and CLIP-170 at microtubule distal ends. *J. Cell Sci.* 112:1437–1447.
Warren, G., and V. Malhotra. 1998. The organisation of the Golgi apparatus. *Curr. Opin. Cell Biol.* 10:493–498.
Waters, M.G., and S.R. Pfeffer. 1999. Membrane tethering in intracellular transport. *Curr. Opin. Cell Biol*. 11:453–459.
Wienke, D.C., M.L. Knetsch, E.M. Neuhaus, M.C. Reedy, and D.J. Manstein. 1999. Disruption of a dynamin homologue affects endocytosis, organelle morphology, and cytokinesis in *Dictyostelium discoideum*. *Mol. Biol. Cell*. 10:225–243.
Williams, B.C., A.F. Dernburg, J. Puro, S. Nokkala, and M.L. Goldberg. 1997. The *Drosophila* kinesin-like protein KLP3A is required for proper behavior of male and female pronuclei at fertilization. *Development (Camb.)*. 124: 2365–2376.
Williams, B.C., M.F. Riedy, E.V. Williams, M. Gatti, and M.L. Goldberg. 1995. The *Drosophila* kinesin-like protein KLP3A is a midbody component required for central spindle assembly and initiation of cytokinesis. *J. Cell Biol.* 129:709–723.
Zalokar, M., and I. Erk. 1976. Division and migration of nuclei during early embryogenesis of *Drosophila melanogaster*. *J. Micro. Biol. Cell*. 25:97–106.
Zarnescu, D.C., and G.H. Thomas. 1999. Apical spectrin is essential for epithelial morphogenesis but not apicobasal polarity in *Drosophila*. *J. Cell Biol.* 146:1075–1086.